Validation of Solid Oxide Cell and Stack Model Using SIMULINK for Gas-Cooled Reactor Analysis

Jiwon Ahn [a], Hyoung Kyu Cho [a*] Byung Ha Park [b]
[a] *Department of Nuclear Eng., Seoul National Univ., 1 Gwanak-ro, Gwanak-gu, Seoul 08826*
[b] *Nuclear Hydrogen Research Team, Korea Atomic Energy Research Institute, 111 Daedeok-daero 989 beon-gil, Yuseong-gu, Daejeon 34057*
**Corresponding author: chohk@snu.ac.kr*

***Keywords : Solid Oxide Electrolysis (SOE), Hydrogen Production, Nuclear Energy.**

1. Introduction

Nuclear power is one of the most reliable energy sources, providing a high energy density and a stable supply of electricity and heat. As a result, global nuclear power capacity has been continuously increasing and is expected to expand further in the future (Fig. 1 (a)).

As the hydrogen economy becomes increasingly important for achieving Net-Zero, global hydrogen demand is expected to rise significantly (Fig. 1 (b)). Currently, hydrogen production methods include reforming and electrolysis, with electrolysis being recognized as a carbon-free and environmentally friendly alternative.

Among electrolysis technologies, Solid Oxide Electrolysis (SOE) is the most efficient, as it operates at high temperatures and utilizes both electrical and thermal energy. This makes it more effective than other methods, such as alkaline and proton exchange membrane electrolysis. Therefore, nuclear-powered SOE-based hydrogen production holds great potential as a sustainable and clean hydrogen supply solution.

In this study, SOE cells and stacks models for a nuclear-powered SOE system are developed and validated experimentally.

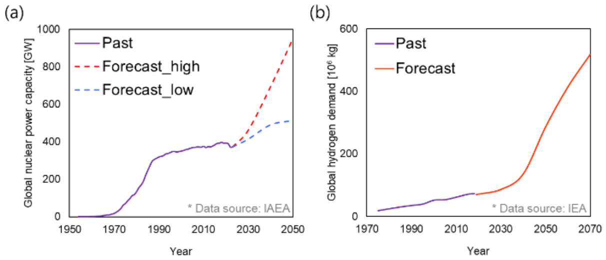

Fig. 1 Past trends and future projections of (a) nuclear power capacity and (b) hydrogen demand.

2. Model descriptions

2.1. Mathematical model

The SOE model consists of three sub-models to analyze the electrolysis process described by Eq. (1): the electrochemical model, the mass conservation model, and the energy conservation model.

$$H_2O_{(g)} \rightarrow H_2 + 1/2\, O_2 \tag{1}$$

The electrochemical model expresses the operating voltage of a cell as a function of current density (i), as shown in Eq. (2). The operating voltage is expressed as the sum of Nernst voltage and various overpotentials.

$$V_{op}(i) = V_{NER} + V_{act} + V_{ohm} + V_{con} \tag{2}$$

Nernst voltage (V_{NER}) represents thermodynamic energy to split steam. The overpotentials consist of activation overpotential, ohmic overpotential, and concentration overpotential. Activation overpotential (V_{act}) represents the energy barrier that must be overcome for the reaction at the catalyst. Ohmic overpotential (V_{ohm}) refers to the resistance between the SOE cell's components and the charges. Concentration overpotential (V_{con}) indicates concentration differences between the flow channel and the reaction site.

Mass conservation is expressed as a sum of the in and out flow rates of each species within a control volume**:**

$$\frac{dn}{dt} = \sum_i \dot{n}_{in,i} - \sum_i \dot{n}_{out,i} \tag{3}$$

where n is mole of all species in a control volume; $\dot{n}_i$ means molar flow rate of species i, respectively.

The amount of species produced or consumed by the electrochemical reaction can be determined using the current. Specifically, the amount of H_2 generated through the electrochemical reaction is given by Equation (4). The amount of H_2O consumed is equal to that of H_2 produced, while that of O_2 generated is half that of H_2 produced.

$$\dot{n}_{react,H2} = \frac{I}{2F} \tag{4}$$

where I and F are current and Faraday constants, respectively.

The energy conservation model expresses the temperature variation of a control volume by considering the heat entering and leaving it. As shown in Equation (5), the heat exchange within a control volume consists of: heat carried by the inlet and outlet flow, heat transfer between control volumes, and heat generated by electrochemical reactions.

$$(\rho V C_v)\frac{dT}{dt} = \sum \dot{Q} \tag{5}$$

where ρ is density; V is volume; C_v is specific heat at constant volume; T is temperature; $\dot{Q}$ is heat flow rate.

The heat generated by the electrochemical reaction is calculated by subtracting the enthalpy difference between reactants and products from the operating voltage, as shown in Equation (6). This is because the enthalpy difference between reactants and products is absorbed as part of the enthalpy of the generated species.

$$\dot{Q}_{react} = \left(V_{op} - \frac{\Delta h_{react}}{2F}\right) I \tag{6}$$

where Δh_{react} is the enthalpy difference between reactants and products.

2.2. Simulation methodology

As shown in Fig. 2, the three sub-models exchange information with each other based on the input data, including the inlet flow rates of each species, the operating voltage, and the initial temperature. After performing calculations, the model outputs the outlet flow rates of each species, the current density, and the temperature of the control volumes.

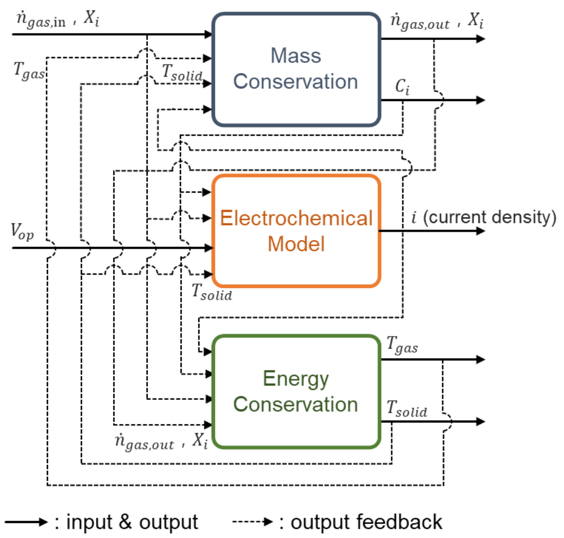

Fig. 2 Computational flowchart for solving the governing equations in the node model.

To enable fast and efficient computation, the SOE stack is structured hierarchically (Fig. 3). The SOE stack model consists of multiple SOE cell models assembled vertically. Within the stack, thermal conduction occurs as temperature information is exchanged between control volumes that are in contact at the inter-connector of adjacent SOE cells.

Each SOE cell model is composed of multiple SOE node models, which are arranged along the flow channels in a cross-flow configuration. Within the SOE cell model, solid control volumes in contact exchange temperature information, leading to thermal conduction. Additionally, solid/gas control volumes exchange temperature information, where convective heat transfer occurs according to Fourier's law. Furthermore, when flow channels are connected, the outlet flow rate and temperature information of a previous node are transferred to the next node based on the flow direction.

To balance computational accuracy and efficiency, this study organizes five node models per flow channel, forming a 5 × 5 cell model [1]. The SOE node model represents the lowest hierarchical level within the SOE cell and SOE stack models, and it follows the computational process outlined in Fig. 2.

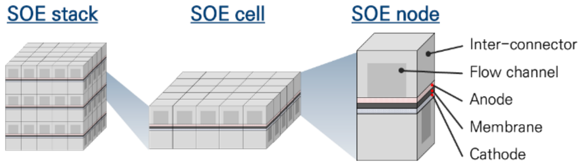

Fig. 3 Structural hierarchy of the SOE stack, cell, and node models.

3. Results

3.1. Verification

To verify the proper implementation of the developed 5×5 cell model, a simulation was conducted under thermo-neutral voltage (1.2867 V at 1073.15 K) using the cell geometry and properties in the literature [2]. The simulation ran for 86400 seconds (24 hours), after which mass and energy conservation were examined at steady state.

Fig. 4 presents the molar flow rates of each species at both the inlet and outlet of the cell. The flow rates of H_2 and O_2 increase at the outlet compared to the inlet, while that of H_2O decreases. That occurs because the electrochemical reaction consumes and generates species as described in Eq. 1. The difference remains at the order of 10^{-18} when compared with the theoretical values from Eq. 4, which are calculated using the current density (1190.095 A/m^2) at the steady state. Therefore, it confirms that the mass conservation is well maintained.

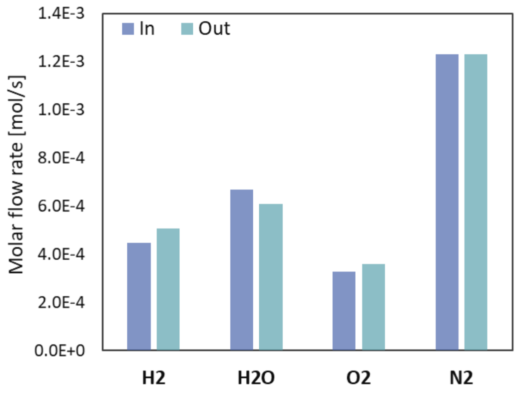

Fig. 4 Species' molar flow rate at inlet and outlet.

Fig. 5 illustrates the temperature distribution of the membrane under thermo-neutral conditions, verifying that the thermo-neutral state is well reproduced. The temperature distribution remains nearly identical to its initial value, confirming that energy conservation is satisfied [2].

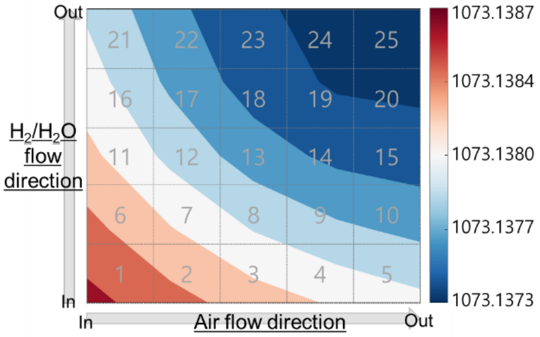

Fig. 5 Temperature distribution of the membrane at thermo-neutral voltage of 1073.15 K.

3.2. Validation

The SOE stack used in the experiment consisted of 30 cells. Certain cell geometries—such as cell size, active area, cathode thickness, and anode thickness—were provided by POSCO HOLDINGS. The exchange current density was estimated based on reasonable values from [3]. Other geometries and properties were obtained from [4]. The details are summarized in Table 1.

Table 1 Geometry and properties of the SOE cell within the SOE stack.

Parameter	Value
Cell size [cm × cm]	12 × 12
Active area [cm × cm]	10 × 10
Exchange current density; anode [A/m²]	2.282e+5
Exchange current density; cathode [A/m²]	7.987e+4
Thickness; anode [㎛]	45
Thickness; cathode [㎛]	680
Thickness; membrane [㎛]	20

Table 2 displays both the experimental conditions and results. The experimental results include the measured voltage and outlet temperature, while the experimental conditions encompass all other.

KAERI conducted a SOEC performance test connecting high temperature helium circulation loop. The experiment was performed on the SOE stack under three different cases, as summarized in Table 2. The experimental procedure proceeded as follows: Prior to applying any load, nitrogen was supplied to the cathode side and air to the anode side, with a heater placed at the top of the stack. The cell temperature was gradually increased at a rate of approximately 1 °C per minute. This slow increase in temperature was crucial to minimize thermal stress and avoid potential cell damage. Once the cell temperature reached the desired initial operating temperature, the fluid supplied to the cathode was replaced with a steam/hydrogen mixture, and an external load was then applied. After confirming hydrogen production, voltage was measured.

Table 2 Experimental operating conditions and results.

Parameter		Case 1	Case 2	Case 3
Condition	Current density [A]	80	80	75
	Initial cell temperature [°C]	730	770	830
	Gas temperature; cathodic inlet [°C]	713	749	807
	Gas pressure; cathodic inlet [$kPa_{(g)}$]	8.32	8.56	9.03
	Gas flowrate; H_2O at cathodic inlet [kg/hr]	4.44	4.38	3.88
	Gas flowrate; H_2 at cathodic inlet [SLPM]	22	26	17
	Gas temperature; anodic inlet [°C]	722	756	813
	Gas pressure; anodic inlet [$kPa_{(g)}$]	6.45	6.1	6.54
	Gas flowrate; air at anodic inlet [SLPM]	75	75	80
Result	Voltage [V]	46.6	41.9	40.4
	Gas temperature; cathodic outlet [°C]	760	785	850
	Gas temperature; anodic outlet [°C]	760	795	860

Fig. 6 presents the average current density and voltage values from both the experiment and the model for each case in Table 2. The experiment used a 30-cell stack, while the model utilized a cell model. To compare, the stack voltage was divided by 30, and the current was divided by the active area to obtain the node's current density. The values for each case were: Case 1: 8000 A/m², 1.553 V; Case 2: 8000 A/m², 1.397 V; Case 3: 7500 A/m², 1.347 V.

The model's average current densities were 8626.88 A/m², 7708.92 A/m², and 8031.93 A/m², with errors of 7.84 %, 3.64 %, and 7.09 %, all within 10 %. Thus, the electrochemical model within the developed cell model is validated.

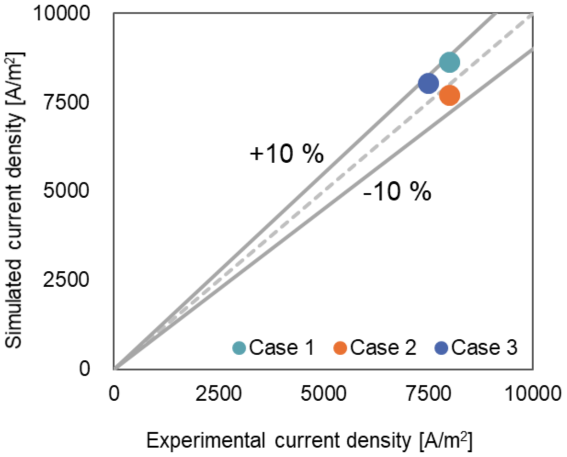

Fig. 6 Comparison of current density of the developed model against experimental data.

The temperatures at the cell outlet were compared. In Table 3, the number of nodes refers to the nodes shown in Fig. 5. In Case 1, the temperature difference between the two inlets in both the experiment and the model is approximately 2 °C, which is relatively small. In Case 2, the model's temperature is close to the average temperature of the two inlets in the experiment. In Case 3, the model's temperature is more than 15 °C lower compared to the temperature difference between the two inlets in the experiment. Based on the transient analysis of the model (Fig. 7), the variation in current density at a constant voltage tends to be slower than that of temperature. This implies, at a constant current density, temperature variations occur more rapidly than voltage fluctuations. If this effect was not fully captured in the experiment, it could have led to a higher-than-expected voltage measurement.

Table 3 Comparison of temperatures at the cathodic and anodic outlets between the experiment and the developed model.

Parameter	Node	Case 1		Case 2		Case 3	
		Exp.	Model	Exp.	Model	Exp.	Model
Cathodic outlet temp. [K]	21	1033.15	1031.88	1058.15	1061.38	1123.15	1102.34
	22		1033.82		1062.74		1103.01
	23		1034.82		1063.55		1111.11
	24		1034.92		1063.83		1111.37
	25		1034.03		1063.54		1111.26
Anodic outlet temp.[K]	5	1033.15	1029.42	1068.15	1059.05	1133.15	1108.21
	10		1032.15		1061.12		1109.60
	15		1033.89		1062.63		1110.59
	20		1034.54		1063.45		1111.14
	25		1034.08		1063.6		1111.29

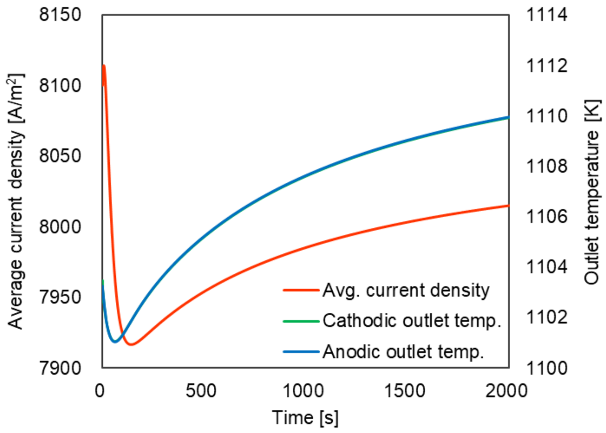

Fig. 7 Transient analysis of average cell current density and outlet temperature at node 25.

4. Conclusion

This study developed and validated a SOE model, incorporating electrochemical, mass conservation, and energy conservation models to simulate nuclear-powered hydrogen production. It was structured hierarchically, with an SOE stack model consisting of SOE cell models, each made up of 5 × 5 node models.

Verification confirmed that mass and energy conservation were properly maintained. Experimental validation showed that its current density predictions deviated from measured values by 7.84 %, 3.64 %, and 7.09 %, while its temperature predictions closely matched experimental data in two cases but differed by over 15 °C in one. That discrepancy is likely due to differences in thermal stabilization time between the model and the experiment.

Overall, this study demonstrates that the developed SOE models effectively capture key electrochemical and thermal-hydraulic phenomena. Future work will be extended to the system scale and connected to nuclear power for energy analysis.

ACKNOWLEDGMENT

This work was supported by the National Research Foundation of Korea (NRF) grant funded by the Korea government (MSIT) (No. 2024-00436693).

REFERENCES

[1] M. Fardadi, F. Mueller, F. Jabbari, Feedback Control of Solid Oxide Fuel Cell Spatial Temperature Variation, J. Power Sources, vol. 195, no. 13, pp. 4222–4233, 2010.
[2] Z. Xia, Z. Deng, C. Jiang, D. Zhao, J. Kupecki, X. Wu, Y. Xu, G. Liu, X. Fu, X. Li, Modeling and Analysis of Cross-Flow Solid Oxide Electrolysis Cell with Oxygen Electrode/Electrolyte Interface Oxygen Pressure Characteristics for Hydrogen Production, J. Power Sources, vol. 529, p. 231248, 2022.
[3] M. Y. Lu, J. G. Railsback, H. Wang, Q. Liu, Y. A. Chart, S. L. Zhang, S. A. Barnett, Stable High Current Density Operation of La0.6Sr0.4Co0.2Fe0.8O3−δ Oxygen Electrodes, J. Mater. Chem. A, vol. 7, pp. 13531, 2019.
[4] S. Lee, H. Kim, K. J. Yoon, J. W. Son, J. H. Lee, B. K. Kim, W. Choi, J. Hong, The Effect of Fuel Utilization on Heat and Mass Transfer within Solid Oxide Fuel Cells Examined by Three-Dimensional Numerical Simulations, Int. J. Heat Mass Transfer, vol. 98, pp. 77–93, 2016.